Follow us @BoneJointOpen

Freely available online OPEN ACCESS

BJO

WRIST & HAND

Assessing the risk of re-fracture related to the percentage of partial union in scaphoid waist fractures

A FINITE ELEMENT STUDY

J. Martin,
N. A. Johnson,
J. Shepherd,
J. Dias

From Leicester General Hospital, Leicester, UK

Aims

There is ambiguity surrounding the degree of scaphoid union required to safely allow mobilization following scaphoid waist fracture. Premature mobilization could lead to refracture, but late mobilization may cause stiffness and delay return to normal function. This study aims to explore the risk of refracture at different stages of scaphoid waist fracture union in three common fracture patterns, using a novel finite element method.

Methods

The most common anatomical variant of the scaphoid was modelled from a CT scan of a healthy hand and wrist using 3D Slicer freeware. This model was uploaded into COMSOL Multiphysics software to enable the application of physiological enhancements. Three common waist fracture patterns were produced following the Russe classification. Each fracture had differing stages of healing, ranging from 10% to 90% partial union, with increments of 10% union assessed. A physiological force of 100 N acting on the distal pole was applied, with the risk of refracture assessed using the Von Mises stress.

Results

Overall, 90% to 30% fracture unions demonstrated a small, gradual increase in the Von Mises stress of all fracture patterns (16.0 MPa to 240.5 MPa). All fracture patterns showed a greater increase in Von Mises stress from 30% to 10% partial union (680.8 MPa to 6,288.6 MPa).

Conclusion

Previous studies have suggested 25%, 50%, and 75% partial union as sufficient for resuming hand and wrist mobilization. This study shows that 30% union is sufficient to return to normal hand and wrist function in all three fracture patterns. Both 50% and 75% union are unnecessary and increase the risk of post-fracture stiffness. This study has also demonstrated the feasibility of finite element analysis (FEA) in scaphoid waist fracture research. FEA is a sustainable method which does not require the use of finite scaphoid cadavers, hence increasing accessibility into future scaphoid waist fracture-related research.

Cite this article: *Bone Jt Open* 2023;4-8:612–620.

Keywords: Scaphoid, Fracture, Partial union, Finite element analysis, Waist fracture, Re-fracture

Introduction

Scaphoid fractures are common in young adults following a fall, with 64% occurring within the scaphoid waist.[1] While established that minimally displaced scaphoid waist fractures can be managed conservatively,[2] the optimal duration of immobilization required for successful conservative waist fracture management is not understood. Premature mobilization before adequate fracture union and stability risks refracture and fracture micromotion, which is theorized to contribute to nonunion.[3] Untreated nonunion usually progresses to scaphoid nonunion advanced

Correspondence should be sent to James Martin; email: james.martin7735@gmail.com

doi: 10.1302/2633-1462.48.BJO-2023-0058.R1

Bone Jt Open 2023;4-8:612–620.

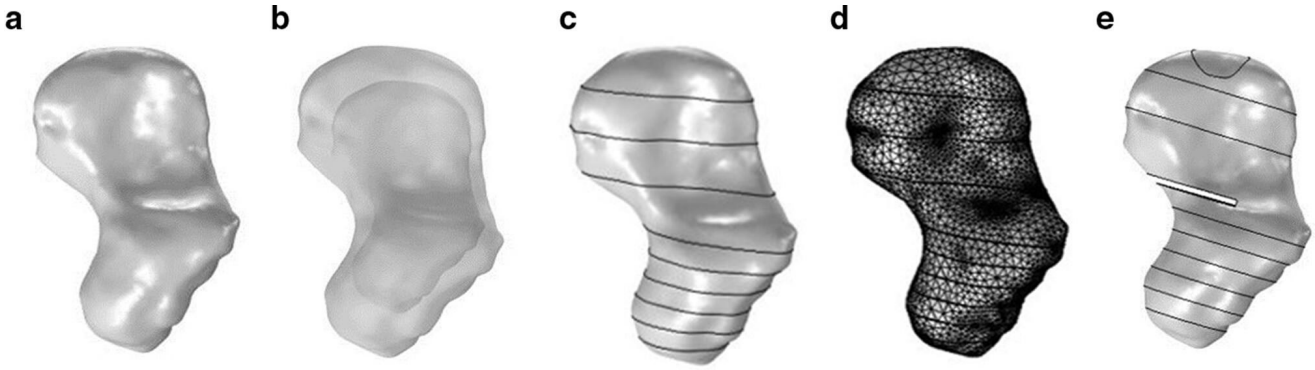

Fig. 1

a) 3D scaphoid model. b) Subchondral and cancellous scaphoid. c) 3D scaphoid model divided into the aforementioned region. d) Scaphoid mesh. e) Finalized fractured scaphoid model. Circle around distal pole represents where the 100 N compressive load was applied.

collapse patterns of arthritis.[4] Conversely, prolonged immobilization can lead to stiffness,[5] delaying return to normal function. These complications are highly detrimental to the social and occupational opportunities of such a young group of patients. This highlights the need to fully understand the degree of scaphoid union required for patients to return to day-to-day functions of the hand and wrist.

Previous studies have attempted to explore the degree of fracture union necessary for patients to commence hand and wrist mobilization. However, the results have varied. Some studies have stated that 50% fracture bridging defines union,[6,7] while Grewal et al[8] previously stated 50% to 75% union defined partial union, with > 75% declared as fully united. Further uncertainty is seen clinically, with Singh et al[9] only advising full return to hand and wrist function in those with at least 75% partial union. Yet on mechanical testing, 25% partial union has shown a low risk of refracture.[10] While rates of nonunion are well established, the risk of refracture is a less well documented, but potentially catastrophic, complication.

Experimental biomechanical musculoskeletal research is often limited by the availability of cadaver specimens. Recently, there has been more focus on the use of computer-based finite element analysis (FEA) to explore fracture-related research.[11-13] While FEA research assessing the stability of surgically fixed scaphoid fractures has been conducted,[14] there is only one recently published paper by Rothenfluh et al,[15] which explored the stability of scaphoid waist fracture partial unions using FEA. However, this paper only explored one fracture pattern, limiting the clinical generalizability of their findings. Therefore, the aim of this study is to assess the risk of refracture in three common scaphoid waist fracture patterns with differing proportions of partial union, using a finite element method (FEM).

Methods

A CT DICOM (digital imaging and communications in medicine) file of a healthy hand and wrist was uploaded into 3D Slicer freeware,[16] enabling generation of a 3D volume-rendered scaphoid model (Figure 1a). A type 1 geometry scaphoid was chosen as this is the most common anatomical variant.[17] The scaphoid model was subsequently uploaded into COMSOL Multiphysics modelling software (COMSOL, Sweden) to enhance the clinical similarity of the scaphoid. Two physiological enhancements were considered: the volume ratio of subchondral to cancellous bone, and the variation in bone mineral density (BMD) throughout the length of the scaphoid.

Ten fractured scaphoid CT scans were obtained from the SWIFFT study data set.[2] Using OsiriX software (Pixmeo, Switzerland), the area ratio between subchondral and cancellous bone of four pre-defined scaphoid regions (proximal pole, proximal waist, distal waist, and distal pole) were collected. A mean value from the four regions was used to create a scaled down cancellous scaphoid (0.746). In COMSOL, a second copy of the scaphoid model was imported and scaled down to match the volume of cancellous bone observed in the data collection (Figure 1b). The same regions were used to collect Hounsfield unit data, which is a measure of the radiodensity of each pixel on a CT scan image.[18] Hounsfield unit values were used for BMD due to their known linear relationship.[18] These values were then converted into elastic modulus, which determines the ease of deformity and fracture in materials.[19] An equation devised for cancellous bone proposed by Morgan et al[20] was used. For subchondral bone, an equation from a histomorphological analysis by Fell et al[21] was deemed appropriate. A Poisson's ratio, which is a measure of material deformation 'in a direction perpendicular to the direction of the applied force', was used for each region.[22] A value of 0.3 was applied, in line with current bone-related literature.[23–25] Subsequently, both the cancellous and subchondral scaphoid were divided into the four aforementioned regions (Figure 1c), enabling application of the specific BMD and elastic modulus values to

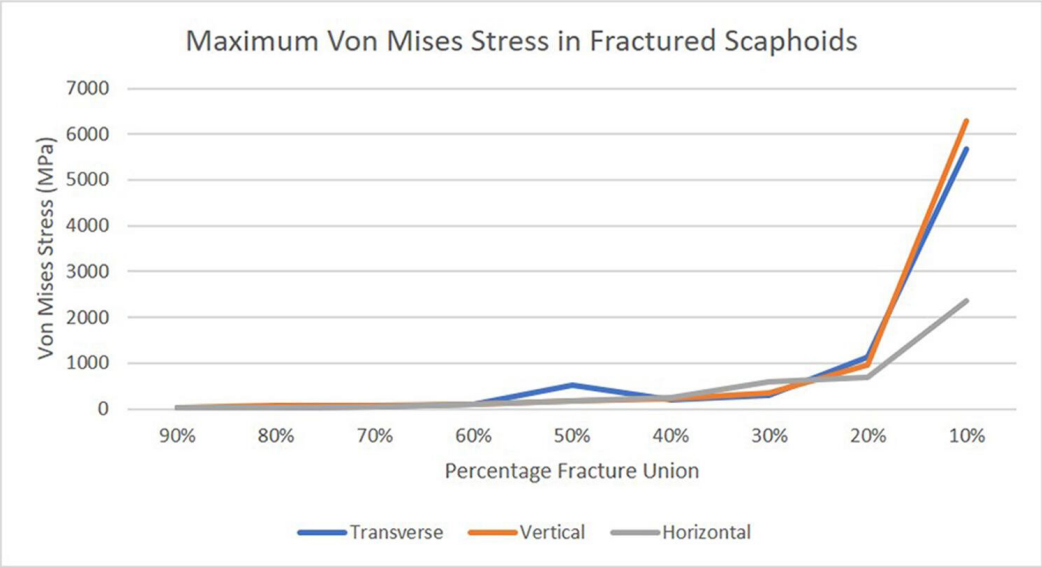

Fig. 2

Maximum Von Mises stress at different stages of fracture union in scaphoid waist fractures stylefix.

their respective domain. An additional three regions were added to graduate both the density and elastic modulus values, reducing the risk of non-physiological, and steep changes between the regions influencing results. Subsequently, a tetrahedral mesh was applied to the model in COMSOL Multiphysics software (Figure 1d), with isotropic bone properties being assumed, enabling FEA to be conducted.

Once the models' physiological enhancements had been applied, artificial waist fractures were generated. Using the Russe classification,[26] three different fracture patterns (horizontal, transverse, vertical) were produced by changing their angle of intersection with the scaphoid's longitudinal axis, which was drawn onto the 3D scaphoid model using known anatomical landmarks.[27–29] This produced three different scaphoid models. A compressive load of 100 N was applied to the distal pole (Figure 1e), replicating the most common physiological force acting upon the scaphoid during normal function.[10,30] This was applied at differing degrees of waist fracture union, ranging from 10% to 90%, with an increment of 10% union. After applying this load, the Von Mises stress was assessed. The Von Mises stress is a theoretical stress that allows comparison between a general 3D stress state and the uniaxial yield stress for a material; it is essentially the stress required to yield or fracture a material.[31] Given the low incidence of plastic deformation in adult bone,[32] analysis of the Von Mises stress through linear elastic FEA was deemed appropriate to assess the risk of fracture.

Results

At 90% and 80% fracture union, the peak Von Mises stress was located away from the site of fracture union, indicating a low risk of refracture. From 70% to 10% partial union, the maximum Von Mises stress was located around the site of union, representing a greater risk of refracture. Table I provides a pictorial representation of the Von Mises stress distribution throughout the scaphoid.

From 90% to 30% partial union, a gradual increase in Von Mises stress was observed (16.0 MPa to 240.5 MPa). However, reducing the degree of partial union to 20% and 10% resulted in a notable increase in Von Mises stress around the site of union. Therefore, while Von Mises stress was focused around the partial union from 70% to 10% fracture healing, the risk of refracture appears greatest from 30% to 10% partial union. An inconsistent value of 509.1 MPa was observed at 50% union in the transverse fracture pattern. Table I does not demonstrate this change due to the opaque scaphoid image; the peak Von Mises stress is within the scaphoid. The 50% fracture ends at a particularly narrow region of the scaphoid model, with a significant geometrical change at the surface, resulting in an inconsistently elevated Von Mises stress at 50% union. Table II and Figure 2 represent the quantitative changes in Von Mises stress.

Discussion

Previous studies have defined 50% scaphoid waist fracture bridging as fully united.[6,7] While this FE study shows this carries a low risk of refracture, the trend in Von Mises stress values from 30% to 90% union indicates that delaying return to activities of daily living for 50% or 75% (as some clinicians prefer) union may be over-cautious, risking stiffness with continued immobilization. The notable rise in Von Mises stress occurred at < 30% union,

Table I. Pictorial representation of von mises stress in scaphoid waist fracture patterns.

Percentage fracture union, %	Scaphoid waist fracture patterns		
	Transverse	Vertical	Horizontal
10	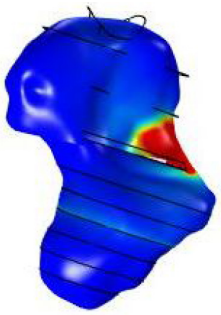	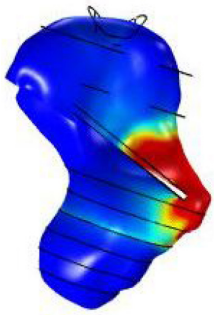	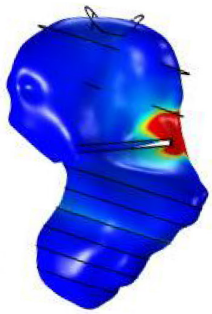
20	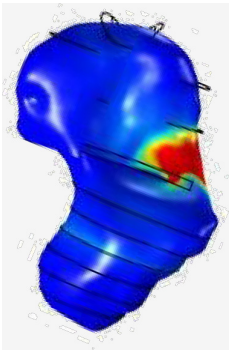	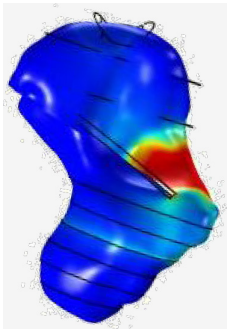	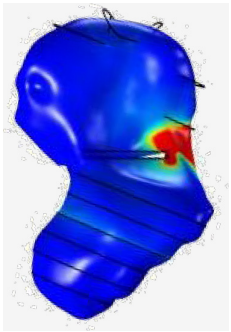
30	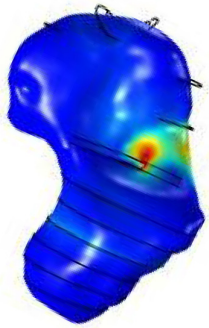	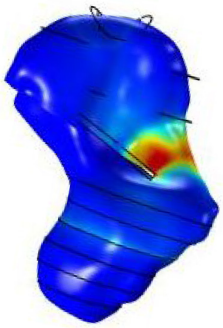	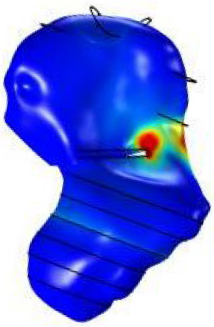
40	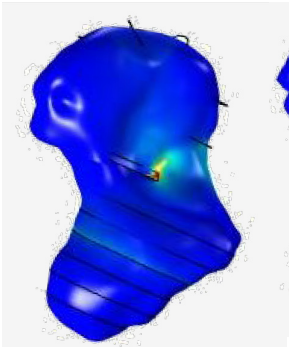	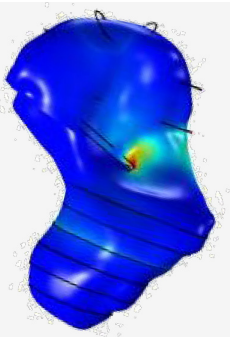	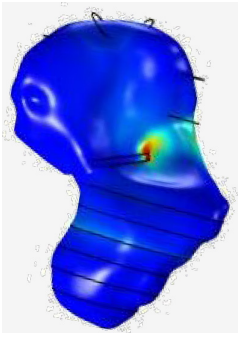

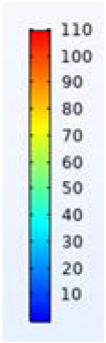

Magnitude of Von Mises Stress (MPa)

Continued

Table I. Continued

Percentage fracture union, %	Scaphoid waist fracture patterns		
	Transverse	Vertical	Horizontal
50		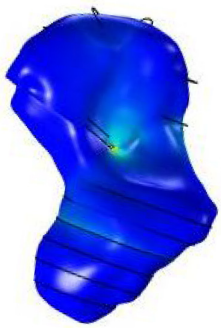	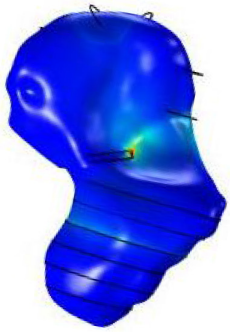
60	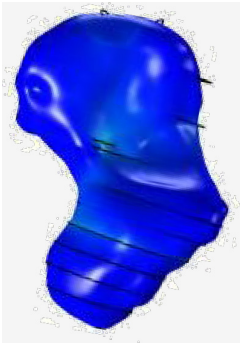	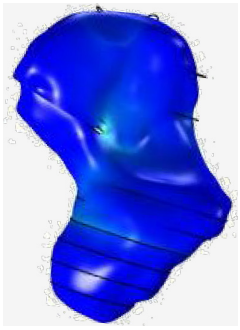	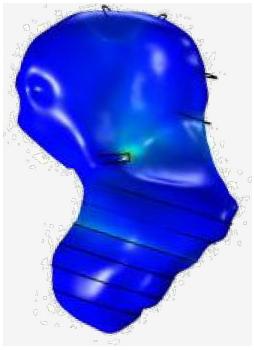
70			
80	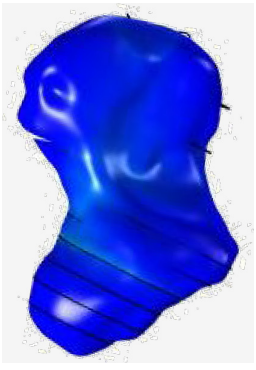		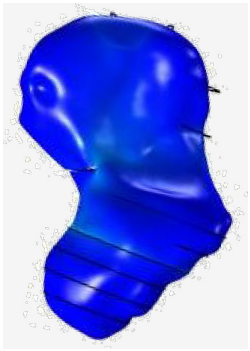

Continued

Table I. Continued

Percentage fracture union, %	Scaphoid waist fracture patterns		
	Transverse	Vertical	Horizontal
90	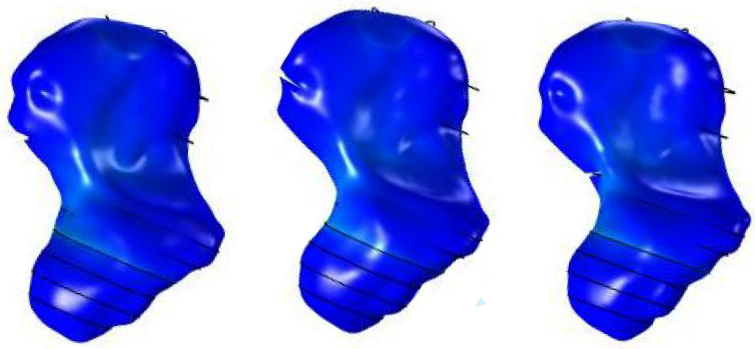		

with this exponentially rising at < 20% union in all three fracture patterns. These findings refute previous biomechanical research by Brekke et al,[10] who investigated the force required to fracture both intact and osteotomized scaphoid cadavers. After applying the same physiological force as this study, no significant difference was observed in the force to fracture intact scaphoids 25%, 50%, and 75% osteotomized scaphoid cadavers. These results differ greatly from this FE study. However, the study by Brekke et al[10] had notable limitations, including not specifying the anatomical variants of the scaphoid used. Additionally, 93% of fractures occurred at the distal pole, which is not in keeping with the reported 10.6% prevalence of distal pole fractures.[1] We identified an increased risk of refracture from 30% to 10% partial union at the site of fracture healing (the region of significant Von Mises stress), highlighting the increased risk of refracture at the fracture site.

Findings from our FE study are more in keeping with work by Guss et al,[14] who assessed the distal pole force required to fracture intact and waist osteotomised scaphoids.[14] The load required for fracture was 610 N in intact scaphoids and 272 N in 50% waist osteotomized scaphoids. Previous literature suggests that the scaphoids most common physiological load is 100 N acting on the distal pole.[10,30] Therefore, as 50% osteotomized scaphoids required 272 N to fracture, it could be argued that 50% partial union is sufficient to return to normal function. This would be in line with our research and other previous studies. Furthermore, Guss et al[14] reported 174 N was required to fracture 75% osteotomised scaphoids, 74 N greater than the most common physiological load. This may be in keeping with the results from our FEA study, as while there was an increase in Von Mises stress from 30% to 20% union, the exponential rise was observed at < 20% union, indicating a greater risk of refracture. Work by Singh et al[9] is also in line with this analysis. Although a small sample size, this paper found that all patients with 25% to 49% partial scaphoid union at eight to 12 weeks progressed to sufficient fracture union and function without reported complication. However, all those with less than 75% partial union in this study were advised against contact sports. This raises the question about what activities should be carried out at certain degrees of fracture union.

Our findings are further validated by the recent paper by Rothenfluh et al,[15] who explored the risk of refracture in scaphoid waist fracture partial unions using FEA, applying the same 100 N load to their scaphoid model. They concluded that 66% scaphoid union was required when fracture healing occurred from the ulnar direction, but only 33% union was required for fractures healing radially. Our fractures healed from the radial direction, indicating similar results. We observed an increased risk of refracture from 30% to 10% partial union, which is in keeping with Rothenfluh et al's[15] recommendation of waiting until 33% scaphoid union is observed. They stated that 25% union was the exact cut-off value for exceeding the ultimate strength of the scaphoid, risking refracture. However, their BMD values came from scaphoid cadavers, which are unlikely to represent the values seen in young adults, in whom these fractures are prevalent. The ultimate strength of the scaphoid was also calculated from these values, with these factors likely to have influenced the Von Mises stresses observed. Furthermore, Rothenfluh et al[15] do not provide data for < 25% union, with our study showing an exponential rise in Von Mises stress from 20% to 10% union. Our FE study builds further on these results, showing no notable difference in refracture risk between the three common waist fracture patterns. This significant finding highlights that our conclusion of the increased refracture risk from 30% to 10% partial union is generalizable to most clinically observed scaphoid waist fractures. Additionally, our

Table II. Maximum Von Mises stress at different stages of fracture union in scaphoid waist fractures.

	Scaphoid waist fractures patterns: maximum Von Mises stress (MPa)		
Fracture union, %	**Transverse**	**Vertical**	**Horizontal**
90	16.1	24.1	16.0
80	16.3	71.2	19.3
70	41.7	70.3	58.0
60	101.5	110.6	98.0
50	509.1	177.8	171.9
40	198.0	230.4	240.5
30	287.0	358.0	584.8
20	1,123.2	956.4	680.8
10	5,670.9	6,288.6	2,353.2

study demonstrates the clear region of refracture risk around the palmar site of fracture union.

There are several strengths to this study. First, it addressed an area of current ambiguity in scaphoid waist fracture research, providing useful clinical information regarding the degree of fracture union required to allow remobilization. This novel methodology does not require the use of finitely available scaphoid cadavers; reusing this method will enable faster progression of research in this field. The external validity of this methodology has been improved by the physiological enhancements applied to the model. FEA studies in this field do not typically consider modelling these enhancements, treating bone as a homogeneous material.[33–35]

There are limitations to this research. Some of the properties of bone could not be modelled due to their complexity. This included using isotropic bone modelling. Bone is anisotropic, meaning its behaviour changes depending on the direction of the applied force.[36] Additionally, linear FEA was performed instead of non-linear FEA, which is more representative of the properties of bone and has been conducted in previous bone-related FEA.[23,37–43] However, studies have demonstrated similar results when using isotropic modelling and linear FEA compared to anisotropic modelling and non-linear FEA, respectively.[44–46] This increased simplicity of FEA improves accessibility into musculoskeletal FE research. However, further properties of bone could not be modelled. The site of fracture union was modelled as healthy adult bone, which would be different to immature woven bone seen during fracture healing. Additionally, there was no consideration of the forces from the scaphoid's surrounding tissues, such as cartilage, muscles, ligaments, and neighbouring bones, which may influence the distribution of Von Mises stress through the scaphoid.

Further work can occur from both the results and methodology demonstrated in this study. Initially, more fracture union analysis should be conducted. A greater variety of waist fracture angulations against the longitudinal axis should be assessed, enabling precise clinical generalizability of results. Furthermore, experimental studies should be conducted to determine the precise stress required to fracture scaphoid partial unions, permitting direct quantitative comparison of Von Mises stress values to refracture risk. This would aid further work in understanding the refracture risk during activities that exert greater loads onto the scaphoid, such as sport and manual labour. Additionally, greater external validity could be achieved by modelling forces acting upon the scaphoid during specific activities, of the kind that Varga et al[47] investigated when exploring hand grasping. This could permit an activity specific return to normal function.

We would recommend that at least 30% union in all three scaphoid waist fracture patterns is observed prior to returning to activities of daily living. This is likely to provide sufficient fracture strength, reducing the risk of refracture. Waiting until 50% or 75% union is unnecessary and increases the risk of post-fracture stiffness. We have also shown a moderate increase in the Von Mises stress from 30% to 20% union. Therefore, it would be sensible to use a splint as additional scaphoid protection if 20% to 30% union is observed.

Take home message

- This finite element study shows that 30% union of scaphoid waist fractures should be observed prior to return to activities of daily living.

References

1. **Garala K**, **Taub NA**, **Dias JJ**. The epidemiology of fractures of the scaphoid. *Bone Joint J*. 2016;98-B(5):654–659.
2. **Dias JJ**, **Brealey SD**, **Fairhurst C**, **et al**. Surgery versus cast immobilisation for adults with a bicortical fracture of the scaphoid waist (SWIFFT): a pragmatic, multicentre, open-label, randomised superiority trial. *Lancet*. 2020;396(10248):390–401.
3. **Erhart J**, **Unger E**, **Schefzig P**, **et al**. In vitro experimental investigation of the forces and torque acting on the scaphoid during light grasp. *J Orthop Res*. 2016;34(10):1734–1742.
4. **Kawamura K**, **Chung KC**. Treatment of scaphoid fractures and nonunions. *J Hand Surg Am*. 2008;33(6):988–997.
5. **Steinmann SP**, **Adams JE**. Scaphoid fractures and nonunions: diagnosis and treatment. *J Orthop Sci*. 2006;11(4):424–431.
6. **Clementson M**, **Jørgsholm P**, **Besjakov J**, **Björkman A**, **Thomsen N**. Union of scaphoid waist fractures assessed by CT scan. *J Wrist Surg*. 2015;4(1):49–55.

7. **Grewal R**, **Suh N**, **MacDermid JC**. Is casting for non-displaced simple scaphoid waist fracture effective? a CT-based assessment of union. *Open Orthop J*. 2016;10(1):431–438.
8. **Grewal R**, **Frakash U**, **Osman S**, **McMurtry RY**. A quantitative definition of scaphoid union: determining the inter-rater reliability of two techniques. *J Orthop Surg Res*. 2013;8(1):28.
9. **Singh HP**, **Forward D**, **Davis TRC**, **Dawson JS**, **Oni JA**, **Downing ND**. Partial union of acute scaphoid fractures. *J Hand Surg Br*. 2005;30(5):440–445.
10. **Brekke AC**, **Snoddy MC**, **Lee DH**, **Richard MJ**, **Desai MJ**. Biomechanical strength of scaphoid partial unions. *J Wrist Surg*. 2018;7(5):399–403.
11. **Orwoll ES**, **Marshall LM**, **Nielson CM**, **et al**. Finite element analysis of the proximal femur and hip fracture risk in older men. *J Bone Miner Res*. 2009;24(3):475–483.
12. **Wong C**, **Mikkelsen P**, **Hansen LB**, **Darvann T**, **Gebuhr P**. Finite element analysis of tibial fractures. *Dan Med Bull*. 2010;57(5):A4148.
13. **Nishida N**, **Ohgi J**, **Jiang F**, **et al**. Finite element method analysis of compression fractures on whole-spine models including the rib cage. *Comput Math Methods Med*. 2019;2019:8348631.
14. **Guss MS**, **Mitgang JT**, **Sapienza A**. Scaphoid healing required for unrestricted activity: a biomechanical cadaver model. *J Hand Surg Am*. 2018;43(2):134–138.
15. **Rothenfluh E**, **Jain S**, **Guggenberger R**, **Taylor WR**, **Hosseini Nasab SH**. The influence of partial union on the mechanical strength of scaphoid fractures: a finite element study. *J Hand Surg Eur Vol*. 2023;48(5):435–444.
16. **No authors listed**. www.slicer.org (date last accessed 29 June 2023).
17. **Pandey VD**, **Singh R**, **Bansal RP**. Study of computed tomographic morphology of scaphoid. *J Anat Sciences*. 2014;1:11–15.
18. **Khan SN**, **Warkhedkar RM**, **Shyam AK**. Analysis of Hounsfield unit of human bones for strength evaluation. *Procedia Materials Science*. 2014;6:512–519.
19. **Zee Ma Y**, **Sobernheim D**, **Garzon JR**. *Schlumberger*Chapter 19 - glossary for unconventional oil and gas resource evaluation and development. In: : 2016.
20. **Morgan EF**, **Bayraktar HH**, **Keaveny TM**. Trabecular bone modulus-density relationships depend on anatomic site. *J Biomech*. 2003;36(7):897–904.
21. **Fell NLA**, **Lawless BM**, **Cox SC**, **et al**. The role of subchondral bone, and its histomorphology, on the dynamic viscoelasticity of cartilage, bone and osteochondral cores. *Osteoarthritis Cartilage*. 2019;27(3):535–543.
22. **Belyadi H**, **Fathi E**, **Belyadi F**. Chapter thirteen - Rock mechanical properties and in situ stresses. In: *Hydraulic Fracturing in Unconventional Reservoirs*. Second Edition. Elsevier, 2019: 215–231.
23. **Yosibash Z**, **Trabelsi N**, **Milgrom C**. Reliable simulations of the human proximal Femur by high-order finite element analysis validated by experimental observations. *J Biomech*. 2007;40(16):3688–3699.
24. **Dawson JM**, **Khmelniker BV**, **McAndrew MP**. Analysis of the structural behavior of the pelvis during lateral impact using the finite element method. *Accid Anal Prev*. 1999;31(1–2):109–119.
25. **Boonyoung C**, **Kwanyuang A**, **Chatpun S**. A finite element study of posteroanterior lumbar mobilization on elderly vertebra geometry. In: *11th Biomedical Engineering International Conference (BMEiCON)*. Chiang Mai, Thailand: 2018.
26. **Russe O**. Fracture of the carpal navicular. Diagnosis, non-operative treatment, and operative treatment. *J Bone Joint Surg Am*. 1960;42-A:759–768.
27. **Guo Y**, **Tian GL**. The length and position of the long axis of the scaphoid measured by analysis of three-dimensional reconstructions of computed tomography images. *J Hand Surg Eur Vol*. 2011;36(2):98–101.
28. **Leventhal EL**, **Wolfe SW**, **Walsh EF**, **Crisco JJ**. A computational approach to the "optimal" screw axis location and orientation in the scaphoid bone. *J Hand Surg Am*. 2009;34-A(4):677–684.
29. **Dean BJF**, **Riley ND**, **McCulloch ER**, **Lane JCE**, **Touzell AB**, **Graham AJ**. A new acute scaphoid fracture assessment method: A reliability study of the "long axis" measurement. *BMC Musculoskelet Disord*. 2018;19(1):310.
30. **Javanmardian A**, **HaghPanahi M**. Iranian Conference Of Biomedical Engineering (ICBME); 3 November 2010. In: IranIEEE, .
31. **No authors listed**. What is von Mises stress? SimScale. https://www.simscale.com/docs/simwiki/fea-finite-element-analysis/what-is-von-mises-stress (date last accessed 29 June 2023).
32. **Tianhao W**, **Yueju L**, **Yingze Z**, **Xirui W**. Plastic deformation of the forearm in adults: an analysis of 30 cases. *J Orthop Surg Res*. 2014;9:117.
33. **Bhardwaj A**, **Gupta A**, **Tse KM**. Mechanical response of femur bone to bending load using finite element method. Recent advances in engineering and computational sciences (RAECS) Mar 6 2014. In: *IEEE*.
34. **Fu L**, **Zhao H-W**, **Zhu Y-X**, **Zou Q**, **Liu C-S**, **Zhao B**. Biomechanics analysis of human proximal femur under four different standing postures based on finite element method. In: *IEEE Symposium on Robotics and Applications*.
35. **Papathanasopoulou VA**, **Fotiadis DI**, **Massalas CV**. Intact and implanted Femur behaviour during walking and Jogging. *23rd Annual EMBS International Conference*. 2001;25–28.
36. **Bankoff ADP**. Biomechanical characteristics of the bone. In: Goswami T, ed. *Human Musculoskeletal Biomechanics*. 2012: 61–68.
37. **Yuan G**, **Weiyi C**, **Zhang X**, **Zhu Y**, **Yibo Z**. Biomechanical analysis of odontoid fracture with different loads by finite element method. In: *2nd International Conference on Bioinformatics and Biomedical Engineering (ICBBE' 08)*. 2018.
38. **Sepehri B**, **Rouhi G**, **Yazdi AA**, **Bahari Kashani M**. *2010 17th Iranian Conference Of Biomedical Engineering (ICBME)*. IEEE, 2010.
39. **Li W-J**, **Guo L-X**. Influence of different postures under vertical impact load on thoracolumbar burst fracture. *Med Biol Eng Comput*. 2020;58(11):2725–2736.
40. **Tsubone T**, **Toba N**, **Tomoki U**, **et al**. Prediction of fracture lines of the calcaneus using a three-dimensional finite element model. *J Orthop Res*. 2019;37(2):483–489.
41. **Guo L-X**, **Li W-J**. A biomechanical investigation of thoracolumbar burst fracture under vertical impact loads using finite element method. *Clin Biomech (Bristol, Avon)*. 2019;68:29–36.
42. **Silva MJ**, **Keaveny TM**, **Hayes WC**. Computed tomography-based finite element analysis predicts failure loads and fracture patterns for vertebral sections. *J Orthop Res*. 1998;16(3):300–308.
43. **Fleps I**, **Guy P**, **Ferguson SJ**, **Cripton PA**, **Helgason B**. Explicit finite element models accurately predict subject-specific and velocity-dependent kinetics of sideways fall impact. *J Bone Miner Res*. 2019;34(10):1837–1850.
44. **Lotz JC**, **Cheal EJ**, **Hayes WC**. Fracture prediction for the proximal femur using finite element models: Part II - nonlinear analysis. *J Biomech Eng*. 1991;113(4):361–365.
45. **Lotz JC**, **Cheal EJ**, **Hayes WC**. Fracture prediction for the proximal femur using finite element models: Part I - linear analysis. *J Biomech Eng*. 1991;113(4):353–360.
46. **Verhulp E**, **van Rietbergen B**, **Huiskes R**. Comparison of micro-level and continuum-level voxel models of the proximal femur. *J Biomech*. 2006;39(16):2951–2957.
47. **Varga P**, **Schefzig P**, **Unger E**, **Mayr W**, **Zysset PK**, **Erhart J**. Finite element based estimation of contact areas and pressures of the human scaphoid in various functional positions of the hand. *J Biomech*. 2013;46(5):984–990.

Author information:
- J. Martin, MBChB (Hons), MSc (Hons), Foundation Year 1 Doctor, Leicester Medical School, University of Leicester, Leicester, UK.
- N. A. Johnson, MBChb (Hons), FRCS (Tr&Orth), PG Cert, PhD, Consultant Hand and Wrist Surgeon, Department of Health Sciences, University of Leicester, Leicester, UK.
- J. Shepherd, PhD (Cantab), MEng (Oxon), Lecturer in Engineering, School of Engineering, University of Leicester, Leicester, UK.
- J. Dias, MBBS, FRCS (Ed) (Ortho), MD, Orthopaedic Surgeon - Hand, Elbow and Shoulder, Academic Team of Musculoskeletal Surgery, University Hospitals of Leicester, Leicester, UK.

Author contributions:
- J. Martin: Investigation, Methodology, Validation, Visualization, Writing – original draft, Writing – review & editing.
- N. A. Johnson: Conceptualization, Project administration, Resources, Supervision, Writing – review & editing.
- J. Shepherd: Methodology, Resources, Software, Supervision, Writing – review & editing.
- J. Dias: Conceptualization, Project administration, Resources, Supervision, Writing – review & editing.

Funding statement:
- The authors disclose receipt of the following financial or material support for the research, authorship, and/or publication of this article: University Hospitals of Leicester Academic Team of Musculoskeletal Surgery (AToMS) research funds.

ICMJE COI statement:
- J. Dias declares National Institute for Health and Care Research Health Technology Assessment grants (e.g. for SWIFFT, DISC), which are unrelated to this work.

Data sharing:
- The data that support the findings for this study are available to other researchers from the corresponding author upon reasonable request.

Ethical review statement:
- Ethical approval was obtained for SWIFFT which allows CT images from the trial to be used for other studies by the research team. SWIFFT was approved by the East Mid-

lands Research Ethics Committee (13/EM/0154). The rest of the experimental study does not require ethical approval.

Open access funding:
- The open access fee for this study was provided by University Hospitals of Leicester Academic Team of musculoskeletal Surgery (AToMS) research funds.

© 2023 Author(s) et al. This is an open-access article distributed under the terms of the Creative Commons Attribution Non-Commercial No Derivatives (CC BY-NC-ND 4.0) licence, which permits the copying and redistribution of the work only, and provided the original author and source are credited. See https://creativecommons.org/licenses/by-nc-nd/4.0/